J|A|C|S
ARTICLES
Published on Web 01/18/2003

Combined QM/MM Study of the Mechanism and Kinetic Isotope Effect of the Nucleophilic Substitution Reaction in Haloalkane Dehalogenase

Lakshmi S. Devi-Kesavan and Jiali Gao*

Contribution from the Department of Chemistry and Supercomputing Institute, University of Minnesota, Minneapolis, Minnesota 55455

Received May 17, 2002; E-mail: gao@chem.umn.edu

Abstract: Combined QM/MM molecular dynamics simulations have been carried out for the dehalogenation reaction of the nucleophilic displacement of dichloroethane catalyzed by haloalkane dehalogenase. The computed chlorine kinetic isotope effects and free energies of activation in the wild-type and the Phe172Trp mutant enzyme are found to be consistent with experiment. In comparison with the uncatalyzed model reaction in water, the enzyme lowers the activation barrier by about 16 kcal/mol. The enormous enzymatic action was attributed to a combination of contributions from a change in the solvation effect and transition state stabilization. The unique features of tryptophan's ability to interact favorably with hydrophobic substrates and to form hydrogen bonds to the leaving group chloride ion at the transition state enable both factors to make significant contributions to the barrier lowering mechanism in the enzyme. This is in contrast to the reference reaction in water, in which hydrogen bonding interactions are weakened at the transition state because of dispersed charge distribution at the transition state relative to that in the reactant and product states.

Introduction

Chlorinated hydrocarbons are highly persistent environmental pollutants, which have been found to be carcinogenic and adversely affect the central nervous system.[1] Bioremediation techniques using enzymatic pathways offer an attractive and inexpensive procedure to remove these potent toxins in a matter of weeks rather than decades.[2] Haloalkane dehalogenases are one class of such enzymes that catalyze the conversion of haloalkanes into the corresponding alcohols and halide ions.[2−5] Remarkably, large-scale applications of microorganisms have been made for treatment of groundwater containing 1,2-dichloroethane.[6] Thus, studies aimed at the understanding of the reaction mechanism and effects of mutations can be helpful to protein engineering.[5,7−12] The large amount of experimental data provide an excellent opportunity for computational study,[13−20] which can yield insight into factors that affect the catalytic efficiency of the enzyme. In addition, effects of mutation on structure and activity and crucial interactions in the enzyme active site can be probed, which may be helpful for designing highly efficient enzymes in bioremediation.

There have been a number of computational studies of the enzyme active site with the substrate dichloroethane (DCE).[13−21] The present study extends these investigations by computing the free energy reaction profile along the reaction path in the enzyme using a combined quantum mechanical and molecular mechanical (QM/MM) method.[22−26] A crucial test of the computational technique is provided by comparing the computed

(1) *National Institute for Occupational Safety and Health* **1978**, *Current Intelligence Bulletin # 25, Publication No. 79-146*, 91−100.
(2) Janssen, D. B.; Scheper, A.; Dijkhuizen, L.; Witholt, B. *Appl. Environ. Microbiol* **1985**, *49*, 673−677.
(3) Wischnak, C.; Muller, R. *Biotechnology*, 2nd ed. **2000**, *11b*, 241−271.
(4) Ridder, I. S.; Dijkstra, B. W. *Cattech.* **2000**, *3*, 126−142.
(5) Franken, S. M.; Rozeboom, H. J.; Kalk, K. H.; Dijkstra, B. W. *The EMBO J.* **1991**, *10*, 1297−1302.
(6) Stucki, G.; Thuer, M. *Environ. Sci. Technol.* **1995**, *29*, 2339−45.
(7) Verschueren, K. H.; Seljee, F.; Rozeboom, H. J.; Kalk, K. H.; Dijkstra, B. W. *Nature* **1993**, *363*, 693−8.
(8) Schindler, J. F.; Naranjo, P. A.; Honaberger, D. A.; Chang, C.; Brainard, J. R.; Vanderberg, L. A.; Unkefer, C. J. *Biochemistry* **1999**, *38*, 5772−5778.
(9) Schanstra, J. P.; Janssen, D. B. *Biochemistry* **1996**, *35*, 5624−5632.
(10) Schanstra, J. P.; Kingman, J.; Janssen, D. B. *J. Biol. Chem.* **1996**, *271*, 14 747−14 753.
(11) Pries, F.; Kingma, J.; Krooshof, G. H.; Jeronimus-Stratingh, M.; Bruins, A. P.; Janssen, D. B. *J. Biol. Chem.* **1995**, *270*, 10 405−10 411.
(12) Kennes, C.; Pries, F.; Krooshof, G. H.; Bokma, E.; Kingma, J.; Janssen, D. B. *Eur. J. Biochem.* **1995**, *228*, 403−407.
(13) Damborsky, J.; Kuty, M.; Nemec, M.; Koca, J. *J. Chem. Inf. Comput. Sci.* **1997**, *37*, 562−568.
(14) Damborsky, J.; Bohac, M.; Prokop, M.; Kuty, M.; Koca, J. *Prot. Eng.* **1998**, *11*, 901−907.
(15) Dombrosky, J.; Koca, J. *Prot. Eng.* **1999**, *12*, 989−998.
(16) Kuty, M.; Damborsky, J.; Prokop, M.; Koca, J. *J. Chem. Inf. Comput. Sci.* **1998**, *38*, 736−741.
(17) Lightstone, F. C.; Zheng, Y.; Bruice, T. C. *Bio. Org. Chem.* **1998**, *26*, 169−174.
(18) Lightstone, F. C.; Zheng, Y.; Bruice, T. C. *J. Am. Chem. Soc.* **1998**, *120*, 5611−5621.
(19) Lau, E. Y.; Kahn, K.; Bash, P. A.; Bruice, T. C. *Proc. Natl. Acad. Sci. U.S.A.* **2000**, *97*, 9937−9942.
(20) Lewandowicz, A.; Rudzinski, J.; Tronstad, L.; Widersten, M.; Ryberg, P.; Matsson, O.; Paneth, P. *J. Am. Chem. Soc.* **2001**, *123*, 4550−4555.
(21) Lightstone, F. C.; Zheng, Y.; Maulitz, A. H.; Bruice, T. C. *Proc. Natl. Acad. Sci. U.S.A.* **1997**, *94*, 8417−8420.
(22) Gao, J.; Xia, X. *Science* **1992**, *258*, 631−5.
(23) Gao, J. *Methods and applications of combined quantum mechanical and molecular mechanical potentials*; Lipkowitz, K. B., Boyd, D. B., Ed.; VCH: New York, 1995; Vol. 7, pp 119−185.
(24) Warshel, A.; Levitt, M. *J. Mol. Biol.* **1976**, *103*, 227−49.
(25) Field, M. J.; Bash, P., A.; Karplus, M. *J. Comput. Chem.* **1990**, *11*, 700−733.
(26) Stanton, R. V.; Little, L. R.; Merz, K. M., Jr. *J. Phys. Chem.* **1995**, *99*, 17 344−17348.

10.1021/ja026955u CCC: $25.00

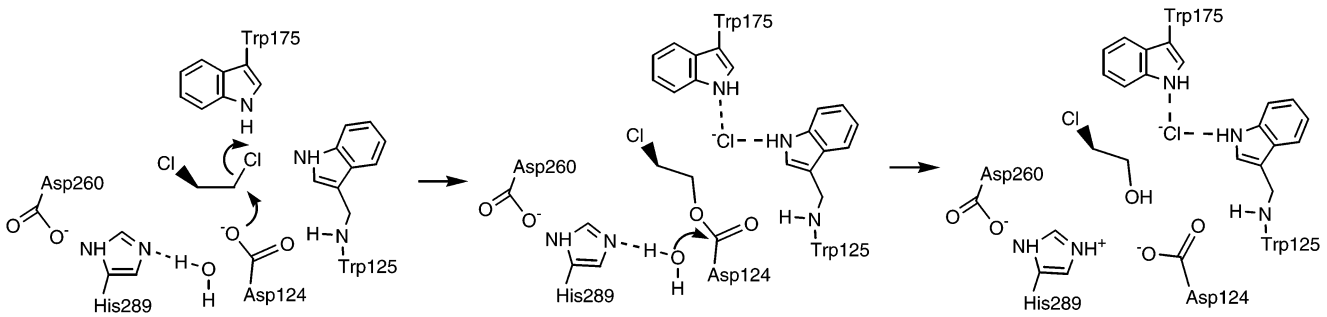

Figure 1. Proposed reaction mechanism for the hydrolysis of dichloroethane by haloalkane dehydrogenase.

free energy of activation and chlorine kinetic isotope effects (KIE) with experiment.[20,27−29] We also examine the effect of residue mutation, specifically the Phe172Trp mutant, on enzyme efficiency. We note that when this work was under review, Shurki et al. reported a study of the dehalogenase reaction, suggesting that the energetic contribution of the near attack conformation (NAC) proposed by Bruice was not significant.[30] The present study provides additional insights on the catalytic mechanism from molecular dynamics and potential of mean force calculations.

Background

Several types of dehalogenases have been identified based on the nature of their substrate specificity. Haloalkane dehalogenases act on haloalkanes,[8,9,20,31−33] haloalkanoate dehalogenases are targeted at halogenated carboxylic acids,[2] and 4-chlorobenzoyl coenzyme A dehalogenases are specific for halogenated aromatic substrates.[34] The enzyme haloalkane dehalogenase (DhlA) from the bacterium *Xanthobacter autotrophicus*, which is a 35 kDa protein consisting of 310 amino acid residues, is used in the present study.[2] DhlA acts on a wide range of substrates, including a number of environmental toxins.[35] Haloalkane dehalogenase is a globular α/β protein, capable of removing the halogen atoms in halogenated hydrocarbons to yield the corresponding alcohols and halides.[31] X-ray crystal structures of the enzyme at 1.9 Å resolution and the enzyme complexed with the substrate 1,2-Dichloroethane at 2.4 Å resolution have been reported.[7,32]

The active site contains a cavity of about 40 Å^3, which is located between two domains of the enzyme.[5] The cavity is predominantly surrounded by hydrophobic residues, including Trp125, Phe128, Leu262, and Leu263 of the first domain and aromatic residues from the second or cap domain, including Phe164, Phe172, Trp175, Phe222, Pro223, and Val226. The only charged residues near the cavity are Asp124, Asp260, and His289.

The first step in the catalytic reaction is an S_N2 reaction, involving the nucleophilic attack by Asp124 on DCE to yield an enzyme-ester intermediate (Figure 1).[32] Bruice and coworkers found that DCE adopts a gauche conformation during the dynamics simulation,[17,18] which is confirmed in the present study. The nonnucleophilic oxygen ($O^{\delta 1}$) of Asp124 is electrostatically stabilized in the Michaelis complex ES by hydrogen bonding interactions with two backbone amide hydrogens.[32] In the product state, the leaving group, chloride ion, forms hydrogen bonds with Trp125 and Trp175.[5,7] The tryptophan mutants exhibited decreased affinity for halide ions, i.e., increased rate for product release, and reduced catalytic activity compared to the wild-type enzyme.[12,36] Interestingly, Phe172 has been proposed to be a residue that interacts with the substrate during the reaction.[7,32] However, the Phe172Trp mutant has a reduced rate in the S_N2 step accompanied by a rate increase in the halide ion release.[9,10,37] In the ester intermediate structure, a crystal water (number 393) was found to donate a hydrogen bond to His289, whereas its oxygen points toward the C_γ atom of Asp124, indicative of the progress of the subsequent ester-hydrolysis step.[5,7,11,32] In this step, water393 is activated by the His289−Asp260 pair, a mechanism that has been found in numerous protease and hydrolase enzymes.[11] To study the role of His289 in the hydrolysis of the ester intermediate, a His289Gln mutant was constructed.[11] Results from these experiments indicated that the mutant enzyme was not catalytically active. However, accumulation of the covalently bound ester intermediate was observed. This provides evidence that His289 is essential for the hydrolysis of the covalent alkylenzyme ester intermediate, but is not involved in the initial nucleophilic attack.[5,9,10,37]

Computational Details

A. Modeling. The X-ray crystal structure of the enzyme−substrate complex (at pH 5 and 4 °C) determined at 2.4 Å resolution (Protein Data Bank code 2DHC) was used as the starting geometry for the wild-type DhlA simulations.[7] To mimic the aqueous environment, we employed the stochastic boundary molecular dynamics (SBMD) simulation technique by using a sphere of preequilibrated water molecules to solvate the enzyme.[38−40] The water sphere was centered at the center-of-

(27) Alhambra, C.; Corchado, J.; Sanchez, M. L.; Gao, J.; Truhlar, D. G. *J. Am. Chem. Soc.* **2000**, *122*, 8197−8203.
(28) Alhambra, C.; Gao, J.; Corchado, J. C.; Villa, J.; Truhlar, D. G. *J. Am. Chem. Soc.* **1999**, *121*, 2253−2258.
(29) Alhambra, C.; Corchado, J.; Sanchez, M. L.; Garcia-Viloca, M.; Gao, J.; Truhlar, D. G. *Journal of Physical Chemistry B* **2001**, *105*, 11 326−11 340.
(30) Shurki, A.; Strajbl, M.; Villa, J.; Warshel, A. *J. Am. Chem. Soc.* **2002**, *124*, 4097−4107.
(31) Keuning, S.; Janssen, D. B.; Witholt, B. *J. Bacteriol.* **1985**, *163*, 635−639.
(32) Verschueren, K. H. G.; Franken, S. M.; Rozeboom, H. J.; Kalk, K. H.; Dijkstra, B. W. *J. Mol. Biol.* **1993**, *232*, 856−72.
(33) Prince, R. C. *TIBS* **1994**, *19*, 3−4.
(34) Benning, M. M.; Taylor, K. L.; Liu, R.-Q.; Yang, G.; Xiang, H.; Wesenberg, G.; Dunaway-Mariano, D.; Holden, H. M. *Biochemistry* **1996**, *35*, 8103−8109.
(35) Janssen, D. B.; Schanstra, J. P. *Curr. Opin. Biotech* **1994**, *5*, 253−259.
(36) Krooshof, G. H.; Ridder, I. S.; Tepper, A. W. J. W.; Vos, G. J.; Rozeboom, H. J.; Kalk, K. H.; Dijkstra, B. W.; Janssen, D. B. *Biochemistry* **1998**, *37*, 15 013−15 023.
(37) Schanstra, J. P.; Ridder, I. S.; Heimeriks, G. J.; Rink, R.; Poelarends, G. J.; Kalk, K. H.; Dijkstra, B. W.; Janssen, D. B. *Biochemistry* **1996**, *35*, 13 186−13 195.
(38) Brooks, C. L., III.; Karplus, M. *J. Chem. Phys.* **1983**, *79*, 6312−25.
(39) Bruenger, A. T.; Brooks, C. L., III.; Karplus, M. *Proc. Natl. Acad. Sci. U.S.A.* **1985**, *82*, 8458−62.

mass position of the substrate dichloroethane (DCE) and the side chain of Asp124. Water molecules that are beyond 24 Å from the origin or within 2.5 Å of protein atoms were deleted. The choice of a 24 Å sphere was a compromise of ensuring adequate solvation at the chemically interesting site of the system and reducing the overall size of the protein−solvent system for computational efficiency, and this type of simulations have been used in numerous applications with great success.

In the case of the mutant enzyme Phe172Trp, the substrate (DCE) coordinates was constructed through docking and energy minimization of residues in the active site because the published crystal structure of the mutant protein (Protein Data Bank code 1HDE) is an apo-enzyme.[37] Specifically, the initial coordinates of DCE were obtained from a best-fit between the wild-type and the mutant structure, which was followed by 100 steps of energy minimization with the DCE coordinates held fixed. Then, we performed a brief minimization (50 steps) of the whole protein system without geometry constraints. All minimizations were carried out using the adopted basis Newton−Raphson (ABNR) method implemented in CHARMM.[41]

B. Combined QM/MM Potential. To describe the bond-breaking and bond-making process in the enzyme, we used a combined quantum mechanical and molecular mechanical (QM/MM) potential. [22−25,42,43] It would be ideal to use ab initio molecular orbital theory or density functional theory in these calculations. However, it is computationally impractical at the present time because free energy simulations must be carried out, which require ca. 10^6 electronic structure calculations.[44] Consequently, semiempirical methods provide the only practical procedure for free energy simulations that employ explicit electronic structure theory. We chose the semiempirical parametrized model 3 (PM3) method in QM calculations.[45] Semiempirical methods, although less systematic than high-level ab initio models that include electron correlation, can still provide important insights on the reaction mechanism, and have been successfully used in numerous enzymatic reactions by several groups.[28,29,46−51]

It is, however, important to verify the performance of the PM3 model. The activation barrier for the S_N2 reaction of acetate ion and dichloroethane in the gas phase has been determined by Maulitz et al.,[21,52] and the results were compared with MP2/6-31+G(d) calculations. At the MP2 level, the predicted barrier height is 23.2 kcal/mol relative to the ion−dipole complex, whereas the PM3 value is 30.5 kcal/mol (Table 1). In this work, we have carried out Gaussian-2 (G2) calculations for this model reaction,[53] which yields a barrier height of 21.3 kcal/mol with the inclusion of zero-point energy contributions. Thus, the PM3 potential overestimates the intrinsic barrier of S_N2 reaction by 7 to 9 kcal/mol, which must be corrected when it is applied to modeling the enzymatic reaction. Although it is possible to reparametrize the semiempirical model to yield a set of specific reaction parameters (SRP) to improve the agreement,[19,54,55] we did not feel that it is essential in the present study because Bruice and co-workers have previously shown that the use of PM3 in dehalogenase reaction can yield reasonable energetic and structural information, provided that the activation energy is reduced by 7 kcal/mol that is overestimated by the PM3 model in comparison with the MP2 result and by 9 kcal/mol in the present G2 value.[21,52]

Table 1. Computed Free Energies of Activation (kcal/mol) for the Model S_N2 Reaction of Acetate Ion and Dichloroethane in the Gas Phase and in Water, and for the Catalyzed Reaction in the Wild-Type Enzyme and the Phe172Trp Mutant

	model reaction			
method	gas phase	water	wild-type	Phe172Trp
PM3	30.5	39.0	23.0	24.5
MP2/6-31+G(d)	23.2[a]	32.0[a] 31.7[b]	15.7[b]	17.2[b]
G2	21.3	29.8[b]	13.8[b]	15.3[b]
expt		29.9[c]	15.3[d]	16.7[d]

[a] Ref 52. [b] Values for condensed phase and enzyme reactions are obtained by subtracting the difference between semiempirical PM3 and ab initio MP2/6-31+G(d) or G2 activation barriers (7.3 or 9.2 kcal/mol) in the gas phase from the results obtained from molecular dynamics simulations using combined QM/MM potentials. [c] Determined at 373 K.[64] See text for discussion. [d] Computed from k_{cat} using transition state theory. Ref. 10,37.

In the combined QM/MM treatment, the residues directly involved in the S_N2 reaction, including the side chain of Asp124 and the substrate DCE are included in the QM representation. The rest of the enzyme residues and water molecules are described, respectively, by the CHARMM22 force field[56] and the three point charge TIP3P model.[57] The generalized hybrid orbital (GHO) method is used to treat the interface between the QM and the MM region.[58,59] A schematic representation of the QM/MM partitioning of the system is shown in Figure 2.

C. Stochastic Boundary Molecular Dynamics. To carry out free energy calculations, molecular dynamics (MD) simulations were performed using stochastic boundary conditions (SBMD).[38,40] This technique allows MD simulations of a region of the enzyme, consisting of the active site residues, a large portion of the protein and the surrounding solvent.[39] It is an efficient, although approximate, approach for reducing the total number of atoms that must be included in the simulation, and hence, minimizing computational costs.[40] In the SBMD method,

(40) Berkowitz, M.; McCammon, J. A. *Chem. Phys. Lett.* **1982**, *90*, 215−217.
(41) Brooks, B. R.; Bruccoleri, R. E.; Olafson, B. D.; States, D. J.; Swaminathan, S.; Karplus, M. *J. Comput. Chem.* **1983**, *4*, 187.
(42) Singh, U. C.; Kollman, P. A. *J. Comput. Chem.* **1986**, *7*, 718−730.
(43) Liu, H.; Zhang, Y.; Yang, W. *J. Am. Chem. Soc.* **2000**, *122*, 6560−6570.
(44) Gao, J.; Thompson, M. A. *Combined Quantum Mechanical and Molecular Mechanical Methods*; American Chemical Society: Washington, DC, 1998; Vol. 712.
(45) Stewart, J. J. P. *J. Comput. Chem.* **1989**, *10*, 209−220.
(46) Truhlar, D. G.; Gao, J.; Alhambra, C.; Garcia-Viloca, M.; Corchado, J.; Sanchez, M. L.; Villa, J. *Acc. Chem. Res.* **2002**, ACS, ASAP.
(47) Liu, H.; Mueller-Plathe, F.; van Gunsteren, W. F. *J. Mol. Biol.* **1996**, *261*, 454−469.
(48) Monard, G.; Merz, K. M., Jr. *Acc. Chem. Res.* **1999**, *32*, 904−911.
(49) Bash, P. A.; Field, M. J.; Davenport, R. C.; Petsko, G. A.; Ringe, D.; Karplus, M. *Biochemistry* **1991**, *30*, 5826−32.
(50) Mulholland, A. J.; Richards, W. G. *ACS Symp. Ser.* **1999**, *721*, 448−461.
(51) Colonna-Cesari, F.; Perahia, D.; Karplus, M.; Eklund, H.; Branden, C. I.; Tapia, O. *J. Biol. Chem.* **1986**, *261*, 15273−8.
(52) Maulitz, A. H.; Lightstone, F. C.; Zheng, Y.; Bruice, T. C. *Proc. Natl. Acad. Sci. U.S.A.* **1997**, *94*, 6591−6595.
(53) Curtiss, L. A.; Raghavachari, K.; Trucks, G. W.; Pople, J. A. *J. Chem. Phys.* **1991**, *94*, 7221−30.
(54) Cunningham, M. A.; Ho, L. L.; Nguyen, D. T.; Gillilan, R. E.; Bash, P. A. *Biochemistry* **1997**, *36*, 4800−4816.
(55) Alhambra, C.; Luz Sanchez, M.; Corchado, J.; Gao, J.; Truhlar, D. G. *Chem. Phys. Lett.* **2001**, *347*, 512−518.
(56) MacKerell, A. D., Jr.; Bashford, D.; Bellott, M.; Dunbrack, R. L.; Evanseck, J. D.; Field, M. J.; Fischer, S.; Gao, J.; Guo, H.; Ha, S.; Joseph-McCarthy, D.; Kuchnir, L.; Kuczera, K.; Lau, F. T. K.; Mattos, C.; Michnick, S.; Ngo, T.; Nguyen, D. T.; Prodhom, B.; Reiher, W. E., III.; Roux, B.; Schlenkrich, M.; Smith, J. C.; Stote, R.; Straub, J.; Watanabe, M.; Wiorkiewicz-Kuczera, J.; Yin, D.; Karplus, M. *J. Phys. Chem. B* **1998**, *102*, 3586−3616.
(57) Jorgensen, W. L.; Chandrasekhar, J.; Madura, J. D.; Impey, R. W.; Klein, M. L. *J. Chem. Phys.* **1983**, *79*, 926−35.
(58) Gao, J.; Amara, P.; Alhambra, C.; Field, M. J. *J. Phys. Chem. A* **1998**, *102*, 4714−4721.
(59) Amara, P.; Field, M. J.; Alhambra, C.; Gao, J. *Theor. Chem. Acc.* **2000**, *104*, 336−343.

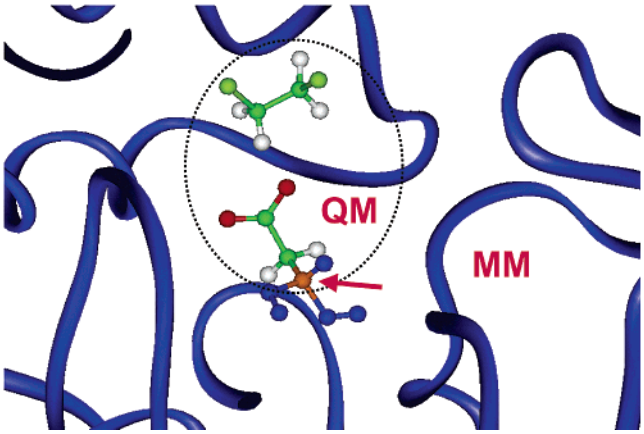

Figure 2. Schematic representation of the partition of the enzyme−substrate-solvent system into a quantum mechanical region and a classical region. The boundary atom is treated using the generalized hybrid orbital method, which is indicated by an arrow.

the whole system is separated into a reaction zone and a reservoir region.[39] The reaction zone is further subdivided into a molecular dynamics region and a buffer region. The dynamics region includes all atoms of the residues that contain any atoms within a radius of 20 Å from the origin of the active site. The buffer region consists of atoms between 20 and 24 Å from the center, and atoms beyond 24 Å constitute the reservoir region, which are held fixed. Atoms in the dynamics region are propagated by Newton's equations of motion, whereas atoms in the buffer region are treated by Langevin dynamics. Protein atoms in the buffer region are constrained by harmonic forces derived from crystallographic temperature factors.[39] A friction coefficient of 200 ps^{-1} for the protein atoms and 62 ps^{-1} for the water molecules are used in the Langevin dynamics.

D. Potential of Mean Force. We use the umbrella sampling technique to compute the potential of mean force (PMF) for the nucleophilic substitution reaction in haloalkane dehalogenase.[60] To overcome the high free energy barrier and to make the computation more efficient, a biasing potential, which ideally corresponds to the negative value of the PMF, is added to the potential energy surface in the molecular dynamics simulation, and is removed in the final statistical analysis. This biasing potential serves the purpose of increasing the probability of sampling high-energy configurations of the system, ensuring effective sampling of the entire reaction path. Because the PMF is not known before the simulation, the biasing potential must be obtained through trial-and-error, which is a shortcoming of the present procedure. However, adaptive umbrella sampling algorithms have been developed, which allow the biasing potential to be updated automatically during the molecular dynamics simulation.[61] The potential of mean force or the free energy reaction profile, $\Delta G(R_\phi)$, as a function of the reaction coordinate is related to the relative probability density $g(R_\phi)$ by

$$\Delta G(R_\phi) = -\frac{1}{\beta}\ln g(R_\phi) + C \qquad (1)$$

where $\beta = (1/k_B T)$, k_B is Boltzmann's constant, T is temperature, and C is a normalization constant. The reaction coordinate R_ϕ is defined as the difference between the bond that is cleaved and the bond that is formed in the S_N2 reaction, i.e., $R_\phi = R(C^1-Cl^1) - R(O^{\delta 2}-C^1)$, with $R(C^1-Cl^1)$ being the distance between the substrate carbon and the leaving group chloride, and $R(O^{\delta 2}-C^1)$ being the distance between the substrate carbon and nucleophile oxygen atoms. The computed PMF was constructed from 14 separate molecular dynamics simulations, which are also called umbrella sampling windows. Each window, which is placed at a position along R_ϕ by an additional harmonic potential (with a force constant of 10 kcal/mol-Å^2), samples the enzyme configuration space in a region of the reaction coordinate near the position of that particular window. Each simulation window consists of at least 50 ps of equilibration and 50 ps of averaging to yield a probability density distribution that is in overlap with those obtained from the two neighboring windows except the two windows in the beginning and the end along the reaction coordinate. Note that the two individual bond distances, C^1-Cl^1 and $O^{\delta 2}-C^1$ are allowed to vary during the dynamics simulation. The PMF was first determined for the S_N2 reaction in the wild-type enzyme. To assess the role of Phe172 for comparison with recent experiments, the reaction profile was also computed for the Phe172Trp mutant. During the SBMD simulation, all bonds involving hydrogen atoms were constrained to their equilibrium distances using the SHAKE algorithm,[62] and the time step used to integrate the equations of motion was 1 fs along with a nonbonded cutoff of 12 Å for both QM/MM and MM interactions. All calculations were performed using a modified version of CHARMM at a temperature of 300 K.[41]

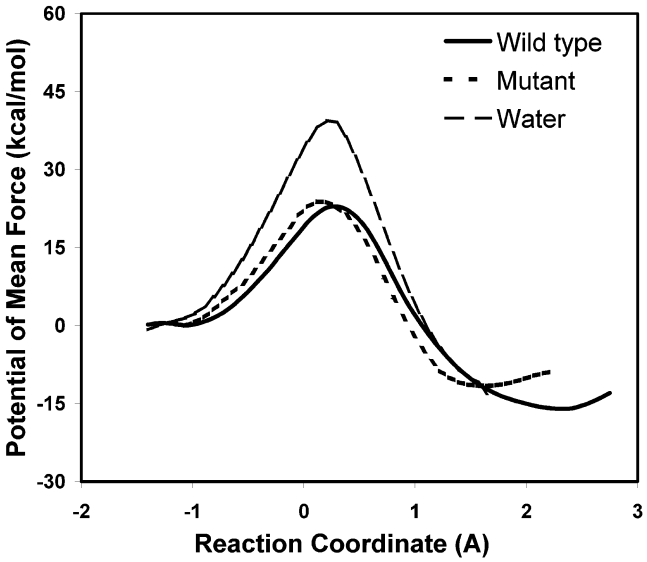

Figure 3. Computed potential of mean force for the nucleophilic substitution reaction between Asp124 and dichloroethane in the wild-type and Phe172Trp mutant haloalkane dehalogenase at 300 K, and for the model reaction of acetate and dichloroethane in water.

Results and Discussion

A. Wild-Type Enzyme. The key results of the present study are shown in Figure 3, which depicts the potentials of mean force for the nucleophilic substitution step in the wild-type dehalogenase enzyme and in the Phe172Trp mutant. In addition, the PMF for the uncatalyzed reaction in water is also displayed

(60) Valleau, J. P.; Torrie, G. M. *A Guide to Monte Carlo for Stastistical Mechanics: 2. Byways.*; Berne, B. J., Ed.; Plenum: New York, 1977; Vol. 5, pp 169−194.
(61) Bartels, C.; Karplus, M. *J. Phys. Chem. B* **1998**, *102*, 865−880.
(62) Ryckaert, J. P.; Cicotti, G.; Berendsen, H. J. C. *J. Comput. Phys.* **1977**, *23*, 327−337.

Table 2. Average Interatomic Distances for Key Residues and the Substrate in the Reactant, Transition State, and Product State for the Wild-type and Mutant Haloalkane Dehalogenase[a]

	wild-type			Phe172Trp		
interaction pair	reactant	TS	product	reactant	TS	product
Asp124 $O^{\delta 2}$−C^1	3.54	1.96	1.45	3.43	2.03	1.43
C^1−Cl (leaving group)	1.83	2.26	3.72	1.82	2.20	3.08
Trp125 $H^{\epsilon 1}$−Cl	4.3	3.3	2.9	3.1	3.0	2.7
Trp175 $H^{\epsilon 1}$−Cl	3.7	2.6	2.5	3.0	2.7	2.8
Phe172 $H^{\delta 1}$−Cl	3.2	3.3	3.3			
Trp172 H^{ζ}−Cl				3.6	3.6	4.2
Glu56 H^N−Asp124 $O^{\delta 1}$	3.0	2.9	3.0	5.0	5.9	6.6
Trp125 H^N−Asp124 $O^{\delta 1}$	3.0	2.9	3.0	3.7	3.7	3.8
Thr173 O^{γ}−Val165 O	4.8	3.7	4.3	6.7	5.0	5.2

[a] Standard errors for average bond distances are about 0.1 to 0.3 angstroms. All distances are given in angstroms.

for comparison. The computed free energies for the enzymatic reactions are all obtained corresponding to the reaction from the Michaelis complex to the enzyme transition state, or the k_{cat} step in the Michaelis−Menten kinetics. From Figure 3 and Table 1, the computed free energy of activation for the displacement of chloride ion by Asp124 in the native enzyme is 23.0 kcal/mol, which represent a lowering of the barrier height by 7.5 kcal/mol from the gas phase value or by 16 kcal/mol from that in aqueous solution. Recall that the PM3 model overestimates the gas phase free energy of activation by 7.3 kcal/mol in comparison with MP2/6-31+G(d) calculations, which is fully transferred into the aqueous and enzyme QM/MM simulations. Taking into account this difference, the corrected free energy of activation for the dehalogenase reaction is 15.7 kcal/mol, which may be compared with the experimental value of 15.3 kcal/mol, derived from the unimolecular rate constant (k_{cat}) at 298 K.[10,37] If the gas phase value obtained from G2 theory was used, the computed barrier height is 13.8 kcal/mol, which is 1.5 kcal/mol smaller than experiment. The reaction is predicted to be exoergic in the enzyme with the ester product being about 16 kcal/mol more stable than the reactant, which indicates that the nucleophilic displacement reaction is essentially irreversible. Indeed, the S_N2 step has been assumed to be irreversible in kinetic studies;[9,10] however, an recent analysis of the chlorine kinetic isotope effects (KIE) indicated that a reversible nucleophilic step would yield a better fit.[20] In the gas phase, we obtained reaction free energies of −9.4, −12.1, and −10.0 kcal/mol at the PM3, MP2/6-31+G(d), and G2 level of theory, respectively. Considering the fact that chloride ion has a slightly greater solvation free energy than an acetate ion, the predicted free energy of reaction in the enzyme is consistent with high-level ab initio and experimental solvation data, and should be quite accurate. Thus, the present theoretical study does not fully agree with the KIE analysis on the reversibility of the nucleophilic reaction step.

The distances, R(C^1−Cl^1) and R($O^{\delta 2}$−C^1), that are used in defining the reaction coordinate are given in Table 2 at different stages during the S_N2 reaction. In addition, average distances for hydrogen bonds that play important roles in stabilizing the substrate along the reaction coordinate are also listed in Table 2. Snapshots of the ES complex, TS and the ester product are shown in Figure 4.

The $O^{\delta 1}$ atom of Asp124 is strongly hydrogen bonded to the backbone amide hydrogens of Glu56 and Trp125 as they are also observed in the crystal structure.[7] The average distance between the nucleophile and substrate ($O^{\delta 2}$ −C^1) is 3.5 Å in the Michaelis complex ES, which is in good agreement with the X-ray crystal structure of the ES complex of the wild-type enzyme. This is consistent with the proposal that $O^{\delta 2}$ is more

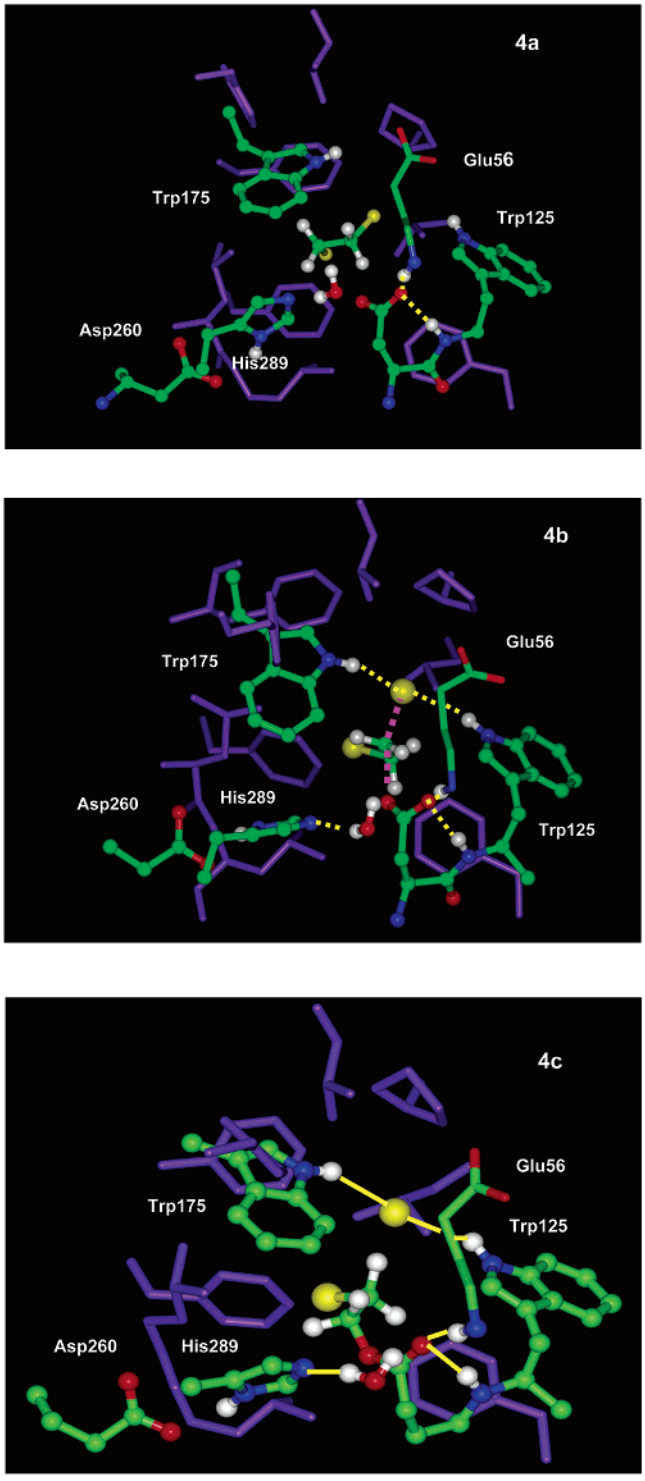

Figure 4. Representative structures for the reactant, transition state, and product complexes in enzyme active site from the last configuration of the window corresponding to their location in the potential of mean force of the wild-type enzyme. These structures are as random as any other configurations sampled during the molecular dynamics simulations. Substrate and key residues that form hydrogen bonds in the chemical step are shown in standard coloring schemes, and hydrophobic residues in the first solvation layer in the active site are shown in purple, including Phe128, Phe164, Phe172, Phe190, Leu179, Pro223, Val226, Leu262, and Leu263.

nucleophilic and acts as the nucleophile in the S_N2 step based on X-ray structural data.[7] The substrate dichloroethane is located in a binding pocket consisting of Trp125, Trp175, Phe172, and a number of secondary hydrophobic residues (Figure 4). The closest average contacts between the leaving group Cl^1 of DCE include the $H^{\epsilon 1}$ atoms of both Trp175 and Trp125 and $H^{\delta 1}$ of Phe172 at distances of 4.3, 3.7, and 3.2 Å, respectively. These interactions render dipolar stabilization to DCE, which is in a gauche conformation.

In the TS region along the reaction path, the distances $R(C^1-Cl^1)$ and $R(O^{\delta 2}-C^1)$ are 1.96 and 2.26 Å, respectively (Table 2, Figure 4b).[63] The three aromatic residues (Trp125, Trp175, and Phe172) form a tripod-like arrangement with the leaving group, Cl^- ion. The most significant change is the shortening of hydrogen-bonding distances by more than 1 Å in going from the Michaelis complex to the transition state between Cl^1 and Trp125 and Trp175. Accompanying these changes are increased hydrogen-bonding interactions between residues Thr173 and Val165 in the cap domain (Table 2), which provide further stabilization of the active site region at the TS of the S_N2 reaction.

The alkylenzyme ester intermediate in the wild-type enzyme is stabilized by hydrogen bonding interactions that are already developed at the TS. The average distances for $R(C^1-Cl^1)$ and $R(O^{\delta 2}-C^1)$ in the ester intermediate are 1.45 and 3.72 Å (Table 2), respectively, which may be compared to values of 1.3 and 4.3 Å observed in the X-ray crystal structure. The chloride ion is hydrogen bonded to two tryptophan residues at distances of 2.5 to 2.9 Å (Table 2). This provides a strong driving force for the formation of the alkylenzyme ester intermediate; however, the stabilizing interactions hinder the release of chloride ion, which are responsible for making that step the rate-determining process in the entire enzyme cycle. Interestingly, a water molecule, which is also found in the crystal structure,[7] is situated near the C^γ atom of Asp124 (Figure 4c) and forms a bridged hydrogen bond with His289. It has been proposed that His289 acts as a proton acceptor to activate the water molecule in the hydrolysis step, which is assisted by electrostatic interactions between the resulting imidazolium cation and Asp260. This charge relay arrangement is analogous to the catalytic triad in serine proteases.

Figure 5 shows the change of partial atomic charges on the nucleophilic carboxylate atoms, the leaving group, chloride ion, and the substrate carbon atom as a function of the reaction coordinate. These charges are obtained by averaging Mulliken population results in molecular dynamics simulations. Clearly, the charge evolution occurs quite early along the reaction coordinate. The transition state is located at a reaction coordinate (R_ϕ) value of 0.23 Å (Figure 3), at which point there is already more than 70% charge separation on the leaving group chloride ion. The two oxygen atoms of the nucleophile Asp124 have similar partial charges (the difference is due to differential polarization through hydrogen bonds) in the reactant state, whereas in the product state, the carbonyl and ester oxygens carry markedly different partial charges. There is an initial increase in charge on the substrate carbon, but it declines as the reaction goes to product.

B. Phe172Trp Mutant Enzyme. The leaving group, Cl^-, of the S_N2 reaction in the wild-type enzyme is stabilized by hydrogen bonding interactions with Trp125 and Trp 175, while

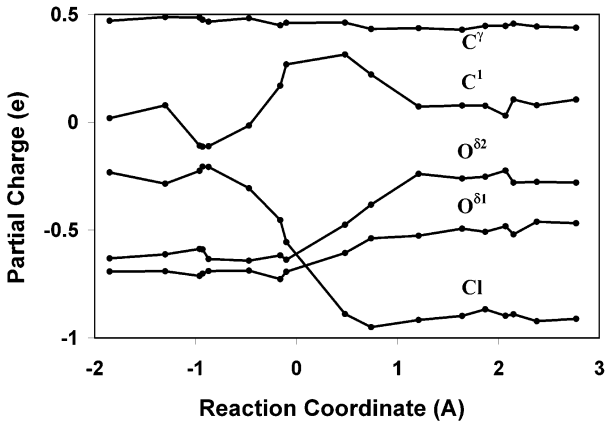

Figure 5. Computed partial atomic charges for the Asp124 carboxylate group and the substrate carbon and leaving group, chlorine atom, along the reaction coordinate.

Phe172 is also in close proximity. One might expect that the Phe172Trp mutation could introduce an additional hydrogen bond to further stabilize the transition state and the product state. However, experimental studies indicate that the Phe172Trp mutant has a higher free enegy of activation than the wild-type by about 1.4 kcal/mol.[37] To provide a rationale for this experimental observation, we have carried out umbrella-sampling free energy simulations of the mutant enzyme using the same simulation protocol as that of the wild-type enzyme. The estimated free energy of activation for the S_N2 reaction in the Phe172Trp mutant enzyme is 24.5 kcal/mol at the PM3/CHARMM level, or 17.5 kcal/mol if the MP2/6-31+G(d) gas-phase result is used. In comparison with the results obtained for the wild-type enzyme, the difference in the calculated activation barrier is 1.5 kcal/mol, in good accord with experiment.[9,37]

The effect of mutation on the activation barrier of the reaction can also be assessed by comparing the interactions in the mutant enzyme with that of the wild-type enzyme (Table 2). Profound changes are observed in the hydrogen bonding interactions between $O^{\delta 1}$ of Asp124 and amide hydrogens of Glu56 and Trp125, resulting in significant effect on the attacking nucleophile, $O^{\delta 2}$ (Figure 6). Depicted in Figure 6 corresponds to the transition state structure of the mutant enzyme. It was surprising to notice that the mutant Trp172 residue is not hydrogen-bonded to the leaving group, but the indole ring points toward the opposite direction to avoid steric congestion with Trp125 and Trp175. The hydrogen bonding interactions between Thr173 and Val165 seem to be disrupted. A distance of 3.7 Å is observed in the TS of the wild-type enzyme, whereas it is changed to 5.0 Å in the mutant (Table 2). This makes a major contribution in destabilizing the TS in the mutant enzyme and an increased rate of chloride release.[9] For comparison, distance between the leaving group chloride ion and the C^1 carbon of the ester product is about 3.1 Å in the mutant and 3.7 Å in the wild-type protein (Table 2). The product in the mutant is less stabilized by about 5 kcal/mol than the wild-type enzyme.

C. Model Reaction in Aqueous Solution and the Origin of Catalysis. For comparison, we have modeled the uncatalyzed S_N2 reaction between acetate ion and dichloroethane in water using the same computational procedures that have been used

(63) Pellerite, M. J.; Brauman, J. I. *J. Am. Chem. Soc.* **1983**, *105*, 2672−80.

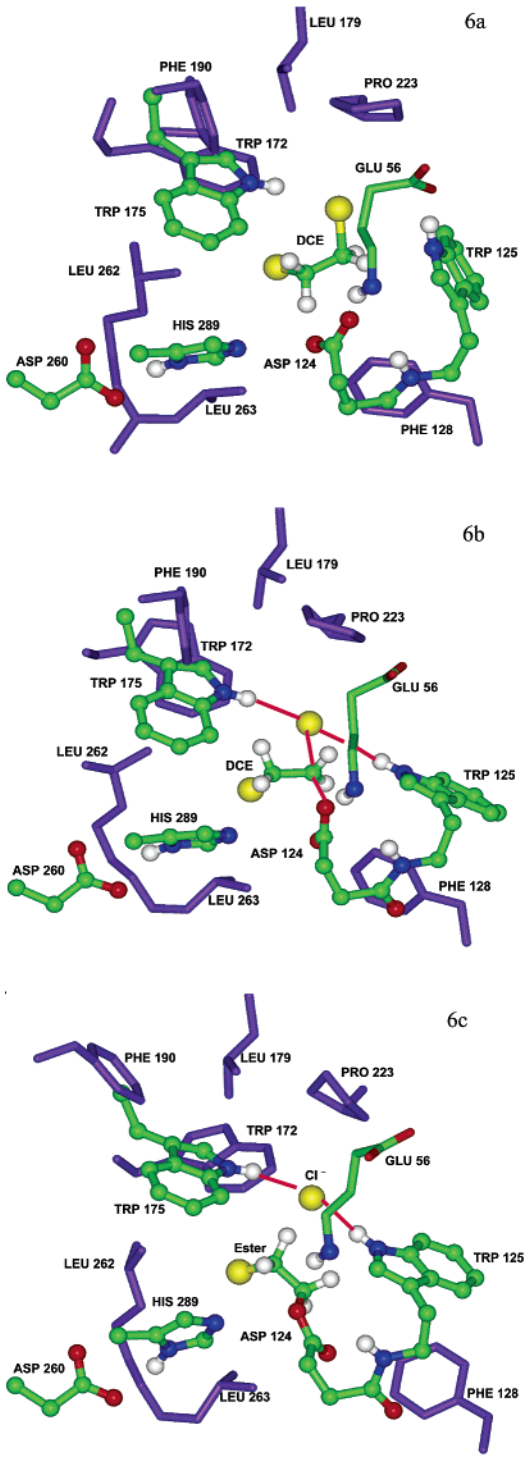

Figure 6. Representative configuration for the reactant, transition state, and product in the Phe172Trp mutant dehalogenase enzyme. All hydrophobic residues are colored in dark purple.

in the enzyme study (Figure 1). The estimated free energy of activation is 39 kcal/mol in water from combined QM/MM umbrella sampling simulations employing the PM3 Hamiltonian for acetate and DCE and the TIP3P model for water. Thus, solvent effects increase the free energy of activation by 8.5 kcal/mol relative to the intrinsic barrier in the gas phase. This finding is in excellent agreement with that obtained by Bruice and co-workers,[18,52] who used the polarizable continuum model to treat the solvent. Recall that the PM3 model overestimates the free energy of activation for the dehalogenase reaction by 7.3 (9.2) kcal/mol compared with MP2/6-31+G* (G2) results. Thus, our best theoretical estimate of the free energy of activation is ca. 30 kcal/mol for the model reaction of acetate ion and DCE in water. In comparison with the enzymatic process, the free energy of activation for the S_N2 step is lowered by 16 kcal/mol in the enzyme than that in water (Table 1). Experimentally, an early study yielded a free energy of activation of 29.9 kcal/mol for the reaction of acetate ion with DCE in water at 373 K,[64] and an extrapolated free energy of activation of 28.2 kcal/mol can be obtained at 300 K using transition state theory. Thus, our theoretical result is in accord with the experimental value of about 28 to 30 kcal/mol. We note that the estimated "experimental" $\Delta G^{\ddagger}$ of 26 kcal/mol, presumably based on the Swain−Scott nucleophilic parameter, in ref 30 was too small.

Several factors contribute to the enzymatic action of barrier lowering. First, there is significant solvent effect on the uncatalyzed nucleophilic substitution reaction in water because the anionic nucleophile is better solvated in polar solvents than the transition state where charge is more delocalized.[65] Further, there is significant energy cost to remove solvent molecules in order for the nucleophile to attack the substrate. The enzymatic process, on the other hand, takes place in a preorganized environment, in which the nucleophile Asp124 and the substrate are already brought together in close contact in the Michaelis complex. The computed average distance between the nucleophilic oxygen of Asp124 and the substrate carbon is 3.5 Å (Figure 4a), in agreement with geometries identified as the near attack conformation (NAC) by Bruice and co-workers.[17−19] The present free energy simulation of the reference reaction between acetate ion and 1,2-dichloroethane in water shows that aqueous solvation effects increase the intrinsic barrier of the nucleophilic substitution by about 8 kcal/mol, providing an upper limit for the role of desolvation in catalysis by haloalkane dehalogenase. For comparison, Shurki et al.[30] found that there is a greater solvation effect of 6.1 kcal/mol in water than that in the enzyme, which is in excellent accord with our estimate. Although these authors do not favor using the term desolvation to describe this effect, they concluded that "the electrostatic solvation effects *increase* the intramolecular barrier for the S_N2 reaction but it does so in a less pronounced way in the enzyme than in water."[30]

The remaining energetic contributions to barrier reduction by the enzyme, which are 8 to 10 kcal/mol, may be attributed to transition state stabilization due to specific interactions of the leaving group with two tryptophan residues. To quantify the stabilizing effects, model calculations for hydrogen bonding interactions between the transition state of the model reaction and an indole ring have been carried out. We obtained an interaction energy of −12.5 kcal/mol using PM3, and −10.5 kcal/mol at the HF/6-31+G(d) level. The corresponding interaction energies are −4.4, and −4.4 kcal/mol, respectively, for the ion−dipole complex of the reactant with an indole molecule. Therefore, each Trp residue can provide transition state stabilization of −6 to −8 kcal/mol, and there are two Trp residues stabilizing the TS in the enzyme. Of course, the alignment of the two dipoles of two tryptophan residues as the partial charge on the chloride leaving group develops during the reaction

(64) Okamoto, K.; Kita, T.; Araki, K.; Shingu, H. *Bull. Chem. Soc. Jpn* **1967**, *40*, 1912−1916.
(65) Chandrasekhar, J.; Smith, S. F.; Jorgensen, W. L. *J. Am. Chem. Soc.* **1985**, *107*, 154−63.

reduces the net gain of interaction energies by one-half of the gain according to linear response theory.[66]

These energetic results suggest that the action of dehalogenase in catalyzing a nucleophilic substitution reaction[67] consists of both features of desolvation effects due to preorganized enzyme environment in the Michaelis complex, and hydrogen bonding stabilization of the transition state from developing specific interactions between the leaving group and tryptophan residues.

In a previous publication, Warshel and Florian[66] criticized the desolvation mechanism proposed by Bruice and co-workers[21] and others[68] on the basis of inspection of the X-ray structure. It was suggested that in the active site of haloalkane dehalogenase, "two dipoles are provided by Trp125 and Trp175, two dipoles by the main chain peptide bonds of Glu56 and Trp125, and two by the end of the α-helix."[66] Indeed, some of these hydrogen-bonding interactions are maintained throughout our molecular dynamics simulation. However, our simulation results of the wild-type enzyme indicate that the side chains of the two tryptophan residues are not directly hydrogen bonded to DCE nor to Asp124 in the reactant state (Michaelis complex), but they are pointed away from the future leaving group chlorine atom. This conformation is preferred because the tryptophan aromatic rings, along with a host of hydrophobic residues (Figure 4), form the major binding pocket for the hydrophobic substrate DCE. This is essential for substrate DCE binding because there is no significant electrostatic interaction between DCE and the enzyme. Furthermore, the newer study by Shurki et al. nicely demonstrated that the protein environment provides smaller solvation effects in the enzyme than in water by 6.1 kcal/mol,[30] which actually supports the idea of significant desolvation effect.

D. Kinetic Isotope Effects. The intrinsic chlorine primary kinetic isotope effect (KIE) for the dehalogenation reaction catalyzed by haloalkane dehalogenase from *Xanthobacter autotrophicus* GJ10 has been determined to be 1.0066 ± 0.0004 experimentally by Paneth and co-workers.[20] To provide additional insights on the dehalogenation reaction, we have computed the primary KIE for the DCE reaction in haloalkane dehalogenase. To calculate the KIE, the ratio of the rate constants between the two different isotope substitutions ($^{35}k/^{37}k$) needs to be evaluated. The potential of mean force calculated for the dehalogenation reaction from classical molecular dynamics simulations in the previous section excludes quantum mechanical vibrational free energies. Although quantum vibrational contributions are not expected to significantly alter the barrier height for reactions involving heavy atom transfer such as the present S_N2 reaction as opposed to reactions involving hydrogen transfer,[69] it is necessary to include these effects to determine the KIE. We used an approach developed recently at Minnesota to include quantum vibrational free energies along the reaction path.[70]

The approach for computing KIEs for enzymatic reactions has been fully described in previous papers,[28,29,46,69] with a focus mainly on proton and hydride transfer reactions. For completeness, we briefly summarize the major computational procedures that are used here. The rate constant corresponding to the nucleophilic substitution reaction from the Michaelis complex to the alkylenzyme intermediate, which is a unimolecular process, at temperature T is written as follows

$$(k)T = \gamma(T)k^{TST}(T) = \gamma(T)\frac{1}{\beta h}e^{-\beta\Delta G^{\ddagger}(T)} \qquad (2)$$

where $\gamma(T)$ is the overall transmission coefficient, k^{TST} is the transition state theory rate constant, $\Delta G^{\ddagger}$ is the free energy of activation, and h is Planck's constant. The free energy of activation $\Delta G^{\ddagger}$ that includes quantum vibrational free energy contributions can be determined from the quasiclassical potential of mean force, which is related to the classical PMF from molecular dynamics simulations by adding the quantum-mechanical vibrational energies for all degrees of freedom except the one corresponding to the reaction coordinate. Thus

$$W^{QC}(R_\phi) = W^{CM}(R_\phi) + \Delta W_{vib}(R_\phi) \qquad (3)$$

where $W^{QC}(R_\phi)$ and $W^{CM}(R_\phi)$ are the quasiclassical (QC) and classical mechanical (CM) potentials of mean force, respectively, and the last term in eq 3, $\Delta W_{vib}(R_\phi)$ is the difference between the quantum and classical vibrational free energies for 3N-7 vibrational modes, where the seventh mode corresponding to the reaction coordinate R_ϕ is projected out of the Hessian with a projection operator.[70] In the present study, we used an instantaneous normal mode approximation[71,72] for a total of 300 configurations, 100 of which from the reactant state (the Michaelis complex), 100 from the TS region and 100 corresponding to the product state, to yield $\Delta W_{vib}(R_\phi)$ for both Cl^{35} and Cl^{37} isotopes.

We then applied an ensemble-averaged variational transition state theory, or EA-VTST,[29,46,69] to estimate the transmission coefficient to account for both the dynamic recrossing and quantum mechanical tunneling contributions associated with the reaction coordinate.[73] In these calculations, we choose the QM region as the primary system in the VTST dynamics trajectory calculations,[74] which is embedded in the field of a static protein environment for each configuration at the location of the transition state along the QC−PMF from molecular dynamics simulations. The computed transmission coefficient is an average result computed for these configurations. To make the computational costs tractable, we considered 10 transition state configurations for these calculations. For each of the 10 configurations, minimum energy paths (MEP) were calculated for isotopes Cl^{37} and Cl.[35] Combining with the TST rate constant, this yields the final EA-VTST rate constant for KIE calculations and the results are listed in Table 3.

Because it is impractical to use high-level ab initio molecular orbital or density functional theory to carry out free energy simulations for enzymatic systems, at least soon, one must rely

(66) Warshel, A.; Florian, J. *Proc. Natl. Acad. Sci. U.S.A.* **1998**, *95*, 5950−5955.
(67) Ingold, C. K. *Structure and Mechanism in Organic Chemistry*; 2nd ed.; Cornell University: Ithaca, New York, 1969.
(68) Dewar, M. J. S.; Dieter, K. M. *Proc. Natl. Acad. Sci. U.S.A.* **1985**, *82*, 2225−2229.
(69) Gao, J.; Truhlar, D. G. *Ann. Rev. Phys. Chem.* **2002**, *53*, 467−505.
(70) Garcia-Viloca, M.; Alhambra, C.; Truhlar, D. G.; Gao, J. *J. Chem. Phys.* **2001**, *114*, 9953−9958.
(71) Ladanyi, B. M.; Stratt, R. M. *J. Phys. Chem.* **1995**, *99*, 2502−11.
(72) Larsen, R. E.; Goodyear, G.; Stratt, R. M. *J. Chem. Phys.* **1996**, *104*, 2987−3002.
(73) Corchado, J. C.; Chuang, Y.-Y.; Fast, P. L.; Villa, J.; Coitino, E. L.; Hu, W.-P.; Liu, Y.-P.; Lynch, G. C.; Nguyen, K. A.; Jackels, C. F.; Gu, M. Z.; Rossi, I.; Clayton, S.; Melissas, V. S.; Steckler, R.; Grarrett, B. C.; Isaacson, A. D.; Truhlar, D. G. 7.9.1 ed.; University of Minnesota: Minneapolis, 1998.
(74) Truhlar, D. G.; Garrett, B. C. *Annu. Rev. Phys. Chem.* **1984**, *35*, 159−89.

Table 3. Calculated Transmission Coefficients, Rate Constants and Chlorine Primary Kinetic Isotope Effect for the Nucleophilic Substitution Reaction in Haloalkane Dehalogenase

substrate	$ClCH_2CH_2(^{35}Cl)$	$ClCH_2CH_2(^{37}Cl)$
$\langle\gamma\rangle$	1.457	1.455
k^{QC} (10^{-5} s^{-1})	8.744	8.725
$k^{EA-VTST}$ (10^{-5} s^{-1})	12.738	12.699
$(^{35}k)/(^{37}k)$	1.0031	
expt	1.0066 ± 0.0005	

on semiempirical approaches in combined QM/MM calculations. It is therefore critical to examine the validity of semiempirical models in these calculations, and the ability to evaluate kinetic isotope effects is a major theoretical development both for the investigation of enzyme mechanism and for the validation of theoretical models to describe transition state in the enzyme. The experimental intrinsic isotope effect for the dehalogenation reaction is 1.0066 from the *n*-BuCl substrate,[20] and it contains information directly relevant to the transition state structure. The chlorine KIE is a small quantity in the absolute sense and is often expressed in terms of percent deviation from unity, i.e., 0.66%, which falls within the range of 0−1% observed for chlorine isotope effects. The computed value of 0.31% from molecular dynamics simulations and EA-VTST theory is smaller than the experimental data by a factor of 2.

The C−O and C−Cl bond distances are predicted to be too short (1.942 and 2.196 Å) at the transition state from PM3 calculations in comparison with the HF/6-31+G(d) results (2.109 and 2.351 Å)[21,52] and the G2 data (2.010 and 2.254 Å). The results from these energy minimization calculations are also reflected in our molecular dynamics simulations, which yield an average C−O distance of 1.95 Å and C−Cl distance of 2.25 Å at the transition state. The structural effect, which favors more covalent character at the TS using PM3, makes the computed KIE underestimated in comparison with experiments and theoretical studies using B3LYP/6-31+G(d) for model systems.[20] Another difference between experiment and our computation study is that the KIE of *n*-BuCl was used to approximate the intrinsic KIE for DCE for the nucleophilic substitution step of the enzymatic process in the experimental analysis. The assumption that the S_N2 step is reversible, which disagrees with the present study may also be a contributing factor to the discrepancy. Although the computed KIE was underestimated by a factor of 2 in comparison with experiment, the results show the sensitivity of KIE on transition state structure and point to a direction where the semiempirical model should be improved for nucleophilic substitution reactions.[19,54,55] Thus, our computational result on chlorine isotope effects is still encouraging.

Conclusions

Combined QM/MM molecular dynamics simulations have been carried out to determine the potential of mean force and the primary kinetic isotope effects for the S_N2 reaction of dichloroethane by Asp124 in haloalkane dehalogenase. The semiempirical PM3 model was used in the description of the reactive potential energy surface for dichloroethane and Asp124, whereas the rest of the system was represented by classical force fields. The computed free energy of activation for the dehalogenation reaction is 23 kcal/mol using the mixed PM3/CHARMM22 potential, and the uncatalyzed model reaction in water has a free energy of activation of 39 kcal/mol. However, previous studies by Bruice and co-workers and the present G2 results show that the PM3 model overestimates the barrier height by 7−9 kcal/mol for the reaction between acetate and dichloroethane in the gas phase. Taking this correction to the PM3 energy into consideration, our best estimate of the free energy barriers are 14 and 30 kcal/mol for the dehalogenation reaction in the enzyme and in water, respectively, in accord with experiments. The enzyme haloalkane dehalogenase lowers the barrier by about 16 kcal/mol compared with the uncatalyzed reaction.

The enormous enzymatic action can be attributed to a combination of desolvation effects and transition state stabilization. The enzyme active site is predominantly hydrophobic except the nucleophilic residue, and the formation of the Michaelis complex brings together the nucleophile Asp124 and the hydrophobic substrate dichloroethane. The difference in free energy of activation between the model reactions in water and in the gas phase provides an upper limit of about 8 kcal/mol from desolvation effects, which is consistent with a value of 6.1 kcal/mol reported by Warshel and co-workers.[30] The remaining 8 to 10 kcal/mol in barrier lowering by the enzyme result from transition state stabilization by increased electrostatic interactions between two tryptophan residues (Trp125 and Trp175) and the partial charges developed on the leaving group at the transition state. This is in contrast to the model S_N2 reaction in water, in which hydrogen bonding interactions are weakened at the transition state because of dispersed charge distribution at the transition state relative to that in the reactant and product state. The unique features of tryptophan's ability to bind hydrophobic residues and to form hydrogen bonds to the chloride ion enable both factors to make significant contributions to the reduction of the activation barrier in the enzyme.

The reaction profile for the Phe172Trp mutant was also computed. It was found that the Phe172 mutation leads to an increase in barrier height by 1.5 kcal/mol, in agreement with experiment. In this case, the small cavity in the active site is not sufficient to accommodate a much larger tryptophan residue, preventing it from forming favorable interactions with the leaving group, and disrupting hydrogen bonding interactions of the chloride ion with Trp125 and Trp175.

The chlorine kinetic isotope effect for the dehalogenation reaction was determined to be 1.0031, which is smaller than the experimental value of 1.0066 ± 0.0005. The underestimated value is mainly due to the use of the PM3 model, which tends to yield shorter C−Cl distances at the transition state, and hence greater covalent character. Nevertheless, the results are encouraging, showing the sensitivity of the computed kinetic isotope effects on transition state structure and the direction in which the semiempirical model may be improved for nucleophilic substitution reactions.

Acknowledgment. The work was partially supported by the National Institutes of Health and the University of Minnesota. We thank Dr. Mireia Garcia-Viloca for helpful discussions and computational assistance, and Professor Donald G. Truhlar for making the POLYRATE program available for the isotope calculations.

JA026955U